Indian Journal of Engineering & Materials Sciences
Vol. 28, February 2021, pp. 102-107

Surface plasmon based fiber optic refractive index sensor

Sakkarai Selvendran[a*], Avaninathan Sivanantha Raja[b], Kadarkarai Esakki Muthu[c] & Srinivasan Yogalakshmi[b]
[a]School of Electronics (SENSE), Vellore Institute of Technology (VIT) University, Chennai, Tamil Nadu 600 127, India
[b]Alagappa Chettiar Government College of Engineering and Technology, Karaikudi, Tamil Nadu 630 003, India
[c]University VOC College of Engineering, Thoothukudi, Tamil Nadu 628 008, India

Received: 18 January 2020; Accepted: 20 April 2020

This paper has proposed a surface plasmon resonance-based photonic crystal fiber (PCF) sensor to detect even a small change in refractive index (RI) values of analytes. The impact on sensor performance by Bezier polygon core structure of the PCF and gold coating in an air hole have been carried out. The sensor resonance wavelength and the respective confinement loss are analyzed for various Bezier polygon parameters and for various gold coating thicknesses. Also, a comparison between gold filling and gold coating in an air hole of PCF have been undertaken to show the superiority of the gold coating in sensor performance. The promising sensor performance has been noted down above the analyte RI of about 1.3 with an upright sensitivity of about 7000 nm/RIU. This type of sensor is of great interest in medical and industrial applications.

Keywords: Surface plasmon resonance, Hollow core photonic crystal fibers, Refractive index, Sensors, Sensitivity

1 Introduction

In recent times, surface plasmon resonance (SPR) has gained a huge momentum in sensing applications. At metal-dielectric interface the applied electromagnetic field induces oscillation of free electrons present in the metal and their oscillation frequency equals the frequency of the applied field. This combined oscillation and its quantum which is termed as surface plasmon, tends to travel along the metal-dielectric interface and achieves its maximum at phase matching condition[1]. The SPR sensing technique exhibits high sensitivity and is being extensively deployed for biosensing.

Photonic crystal fibers (PCFs) are fabricated by periodically perforating the silica material and thereby creating air holes which run along the entire fiber length. They possess exceptional properties like limitless single mode operation, high degree of birefringence, enhanced design flexibility and small size[2]. The PCF based SPR sensors are developed by selectively infiltrating the air holes with liquid and active plasmonic material. They showcase wide sensing range, remote sensing, simple to measure characteristics and they are comparatively inexpensive to fabricate. These sensors have revolutionized the field of fiber optics sensors and are being progressively used in medical diagnostics for detection of various bio-chemicals and organic fluids[3,4].

The initial experiment on bio-sensing and gas detection using SPR was demonstrated in 1983 by Liedberg *et al.*[5]. Later in 2012, Zhou *et al.*[6] carried out numerical simulations for a PCF-based sensor and reported the measurement range of analyte index of the sensor as 1.25 to 2.75. Shuai *et al.*[7] presented a large range detection multi-core holey fiber plasmonic sensor with high linearity and its average sensitivity was determined to be 2929.39 nm/RIU in the sensing range 1.33-2.72 and 9231.27 nm/RIU in 2.73-1.53. Further in 2013, Lu *et al.*[8] designed a polymer PCF based SPR sensor with metal nanowires having a large mode area and determined its spectral and intensity sensitivity to be $8.3 \times 10^{-5} – 9.4 \times 10^{-5}$ RIU. The nanostructured hollow core PCFs (HCPCF) which are greatly appreciated for light guidance by their inherent photonic band gap effect have set a benchmark in the domain of optical fibers. As the light is guided through the central air core of HCPCF, they can be used to manufacture fibers with operating wavelengths that are not supported by the transparent materials. Jiang *et al.*[9], designed the first soft-glass HCPCF with large mode area. They made it using a high-index lead-silicate glass and fabricated it by the stack-and-draw technique. Their soft-glass HCPCF[9]

*Corresponding author (E-mail: selvendrans@aol.com)

was guiding light in 750 to 1050 nm wavelength range with a low loss of 0.74 dB/m. Nannan Luan *et al.*,[10] demonstrated a surface plasmon resonance sensor based on D shaped micro-structured optical fiber with hollow core. T Biswas *et al.*[11], showed that the sensitivity of HCPCF plasmonic sensor with gold as plasmonic material had higher sensitivity compared to silver[11]. PCF based biosensors were also reported by different authors to detect different parameters such as pH, glucose, etc. of bio-analyte[12-18] and cancer cell[19] at various parts of human body like breast, cervical and basal cells.

The guiding light must be coupled enough between the metal surface and analyte amalgam to ensure the accuracy of the PCF sensor[20]. By filling the analytes in the Bezier polygons, the HCPCF sensing effect with higher efficiency is possible. Therefore, instead of using circles, Bezier polygons are introduced in the PCFs. The Bezier polygon structure in the fiber core region[21] lets the Dirac frequency of operation. Dirac mode effects in free lateral confinement and they enable long-range interaction between multiple cores. This property could lead to the creation of new coupling and sensing properties for use in optical couplers, laser arrays, and fiber sensors.

In this paper, a HCPCF sensor is proposed, which is extremely sensitive to small variations in the refractive index (RI) of the analytes. It permits detecting the various types of analytes RI in the early stages, including medical applications. In medical field, it can enable a higher chance of curing the patient in primitive stages rather than starting the treatment in the advanced stages. Here the analysis is carried out to measure the influence of Beizer polygonal fiber core structure in a HCPCF sensor. Also, the impacts of gold coating and gold filling in surface plasmon effect is verified.

2 Structure and basic theory

Here, we have proposed two HCPCF structures which can act as biosensors depending on the gold placement. Figure 1a shows the schematic diagram of the HCPCF with gold filled air hole and Fig. 1b shows the schematic diagram of the HCPCF with gold coated air hole. The diameter (d_1) of the air holes embedded in base silica material is 2.603 μm while the distance between the centers of adjacent holes p is 2.7 μm.

This HCPCF can be used to sense the refractive index (RI) of analyte placed in core, by filling one of the airholes with active metal gold which induces surface plasmons at its surface. The light propagating in core excites the free electrons in adjacent gold wire and they form plasma waves at gold surface. This results in transmission loss of core mode and the

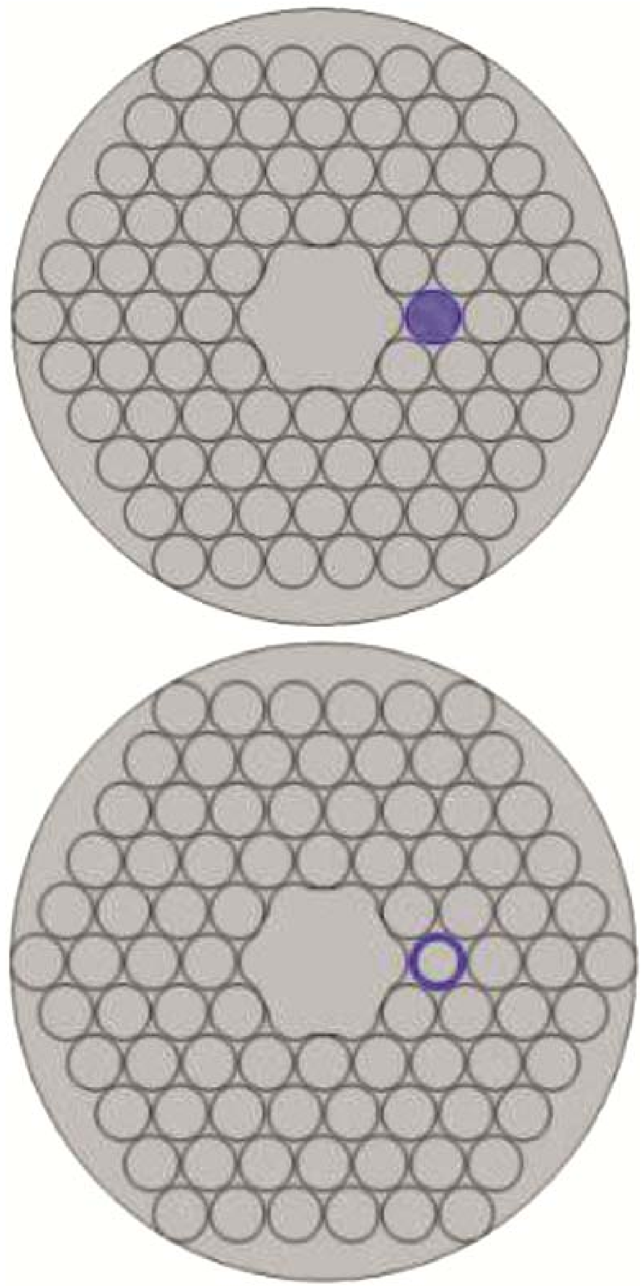

Fig. 1 — Schematic diagrams of the (a) HCPCF sensor with gold filled nanowire (the shaded circle indicates gold nanowire and analyte is placed in the central core region surrounded by air holes) and (b) HCPCF sensor with gold coated air hole.

ensuing loss factor attains its maximum when the phase matching condition is agreed between the light wave and the plasmon wave. This peak resonance occurs at certain wavelength for a specific value of analyte RI. The resonance wavelength shifts upon changing the core analyte RI thereby efficiently sensing small variations in analyte RI values. Simulative analysis are performed using finite element method. A perfectly matched layer of thickness 5 µm is added in order to prevent scattering losses.

The RI of gold, being used as the plasmonic material, is calculated from its permittivity value described by Lorentz-Drude Model[22]. The wavelength dependent RI of silica is calculated using the Sellmeier Equation (1) as stated below[23].

$$n(\lambda)^2 = 1 + \frac{B_1\lambda^2}{\lambda^2 - \lambda_1^2} + \frac{B_2\lambda^2}{\lambda^2 - \lambda_2^2} + \frac{B_3\lambda^2}{\lambda^2 - \lambda_3^2} \qquad ...(1)$$

The constants B_1, B_2, B_3, λ_1, λ_2 and λ_3 are Sellmeier coefficients while λ is wavelength of operation.

3 Results and Discussion

3.1 HCPCF Sensor using Gold filled nanowire

The illustrated HCPCF in Fig. 1a effectively senses liquids having RI above 1.3 and its loss spectrum which is shown in Fig. 2a is arrived at by evaluating the confinement loss of the core mode for different wavelengths ranging from 1.5 to 1.8 µm. The confinement loss factor is calculated from the imaginary part of the effective index value using the following (2) expression[24]:

$$\alpha_L = 40 * \frac{2\pi}{\lambda} * \mathrm{Im}(n_{eff}) \qquad ...(2)$$

where, α_L is confinement loss, λ is operating wavelength and $\mathrm{Im}(n_{eff})$ is the Imaginary value of effective mode index. Finite element method is used to obtain the effective mode index of core mode.

Sharp peaks are observed in loss spectrum for analyte RIs of 1.3 and 1.31 at the resonance wavelengths of 1.64 µm and 1.58 µm respectively. The resonance wavelength for RI of 1.305 occurs at 1.61 µm. The maximum confinement losses of 233.35 dB/cm and 210 dB/cm are obtained for core RI values of 1.3 and 1.31 respectively. Thus as the RI value of analyte in core changes from 1.3 to 1.31, a decreased resonance behaviour occurs accompanied by a blue shift in resonance wavelength.

Figure 2b depicts the variation of real and imaginary parts of the effective index as a function of wavelengths for core RI value of 1.3. The real part of effective index decreases with increase in wavelength and at the resonance wavelength there is a sharp increase in the real part value which thereafter decreases gradually. The real part of the effective index is used in the analysis of dispersion parameters of the proposed structure. The imaginary value attains its maximum at the resonance wavelength and then it tends to decrease forming a bell shaped curve. This curve resembles that of observed confinement loss since confinement loss is directly proportional to imaginary value of effective mode index. The maximum light coupling occurs from the core guided mode to the gold

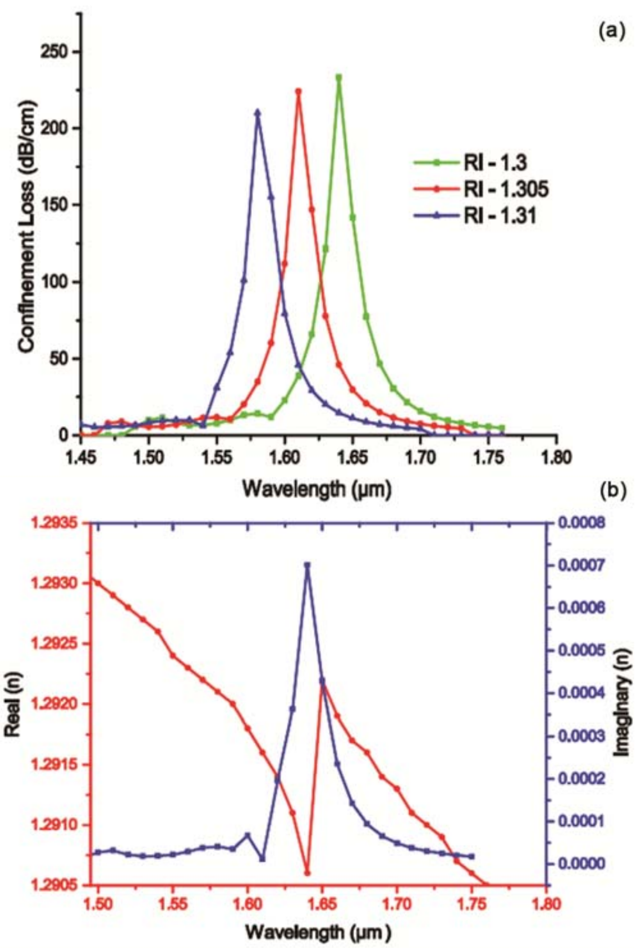

Fig. 2 — (a) Confinement loss variation with respect to wavelength and (b) peak resonance portrayed in terms of real and imaginary parts of effective mode index for analyte RI of 1.3.

filled air hole at the peak resonance wavelength of 1.64 μm which is shown in Fig. 3.

The vital performance parameter of a sensor is its sensitivity. The variation of peak resonance wavelength as a function of the analyte RI value is plotted to obtain the sensitivity curve as shown in Fig. 4. The loss values for different wavelengths are determined and the highest loss value occurs at the resonance wavelength. The resonance wavelength as a function of the analyte RI is plotted and sensitivity of the HCPCF is calculated from this graph using the following Equation (3)[11]:

$$S_{\lambda} = \frac{d(\lambda_{peak}(n_a))}{dn_a} \quad ...(3)$$

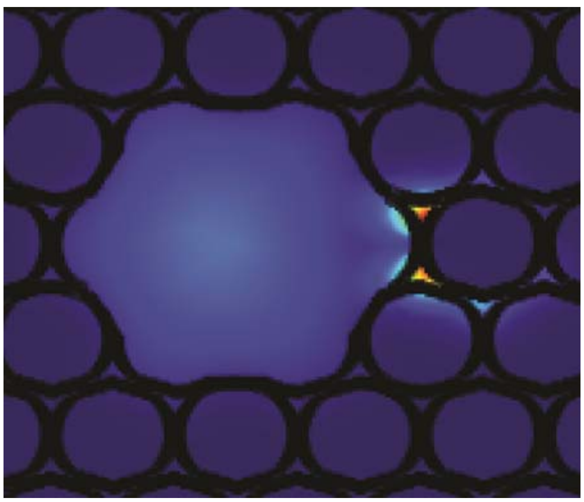

Fig. 3 — Simulation output for maximum resonance for gold filled structure @ 1.64 μm.

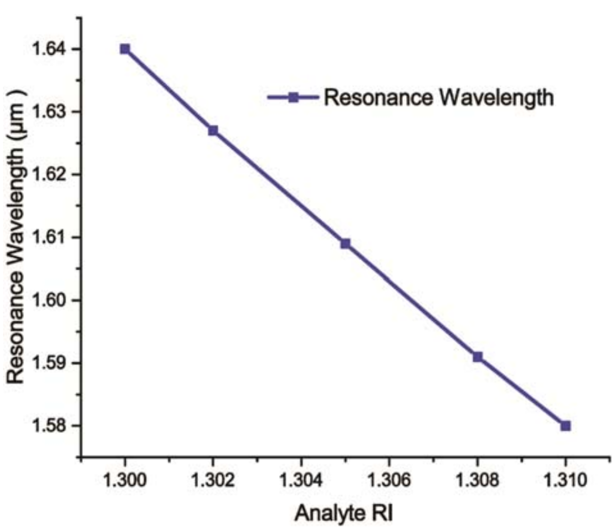

Fig. 4 — Wavelength sensitivity of HCPCF sensor detecting analyte RIs from 1.3 to 1.31.

where, S_{λ} is sensitivity in $nmRIU^{-1}$, λ_{peak} is resonance wavelength (nm) and n_a is RI of analyte. The sensitivity of given HCPCF with gold as plasmonic material is calculated to be 7000 nm RIU^{-1}.

3.2 Impact of Bezier polygon parameter of core on sensing characteristics

The structural parameters of HCPCF control its sensing characteristics. A Bezier polygon is designed in the central core region. This polygon is constructed by specifying linear segments and the control points. The control point is calculated using the control parameter p1 to manipulate the Bezier curve. As the polygon parameter p1 changes, it alters the core area and brings out variations in resonance wavelengths and loss factor values as indicated in Fig. 5. A maximum value of 4 can only be used for the designed HCPCF. When p1 is increased from 3.5 to 4, enhanced resonance takes place due to increased core region and the resonance wavelength shifts by 0.07 μm towards shorter wavelengths. When p1 = 3.5, a peak loss value of 207.25 dB/cm is obtained at 1.71 μm wavelength. While for p1 = 4, at 1.64 μm the maximum loss value of 241.7 dB/cm is observed.

3.3 HCPCF Sensor using Gold coated air hole

In the proposed HCPCF, the gold filled nanowire is replaced by a gold coated air hole in which gold is coated in the inner surface of the air hole as shown in Fig. 1b. For this modified structure, the core RI is 1.3, Bezier polygon parameter (p1) is 4, outer diameter and inner diameter of gold coated air hole being $d_1/2$ and $d_1/2.5$ respectively. Peak resonance occurs at the

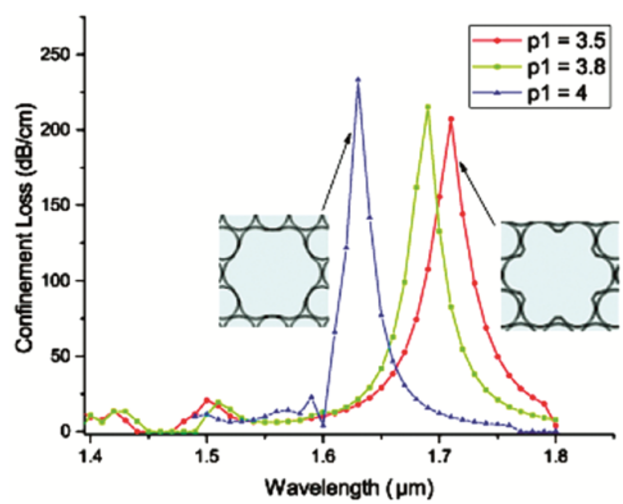

Fig.5 — Confinement loss spectra for analyte RI 1.3 with increasing bezier polygon parameter.

wavelength of 1.72 μm as shown in Figs 6 and 7a. When compared with gold filled nanowire structure, the resonance wavelength occurs at a longer wavelength. It can be observed that the confinement loss factor for the gold coated structure is 269.64 dB/cm, which is greater than the gold filled nanowire structure by 33 dB/cm, and hence an increased resonance occurs for the modified structure. However the sensing behaviour is similar to the former structure only. As shown in Fig. 7b, the peak loss for analyte RI value of 1.31 is 167.26 dB/cm at the resonance wavelength of 1.66 μm which demonstrates a blue shift in resonance wavelength and a decreased resonance wavelength for analyte's RI variation from 1.3 to 1.31. This coated structure proves itself superior to the earlier one by exhibiting increased resonance and also by being economical with lower consumption of gold, the plasmonic material.

Further it is interesting to note from Fig. 7c that the resonance phenomenon gets enhanced on increasing the thickness of the gold coating. The loss value increases with a corresponding blue shift in resonance wavelength when the inner diameter of the gold coated air hole is decreased (which implies that the coating thickness is increased) from $d_1/2.3$ to $d_1/2.7$. Thus optimum resonance occurs at typical thickness value of $d_1/2$ to $d_1/2.7$ having peak loss of 304.7 dB/cm at 1.7 μm. But the increase in CL is observed only till this specific thickness value, after which it deteriorates. Beyond the thickness of $d_1/2$ to $d_1/3.5$, with a confinement loss of 184.82 dB/cm at resonance wavelength of 1.66 μm, no sharper peaks are observed. The underlying fact is that the electric field exists only up to the skin depth and it is evanescent in nature. Hence no significant increase in resonance behaviour will be observed even when the gold thickness is increased beyond the skin depth value.

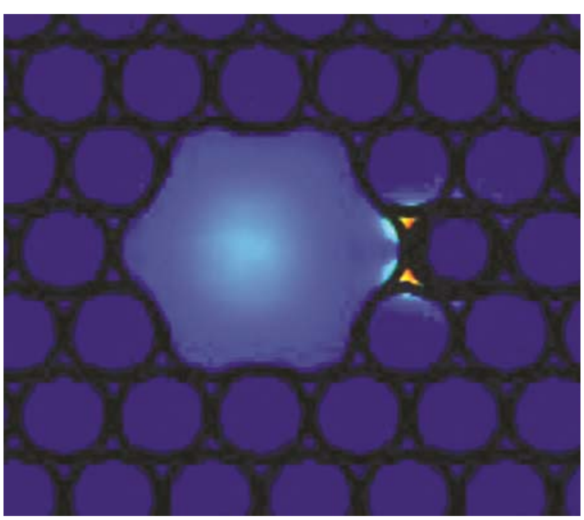

Fig. 6 — Simulation output for maximum resonance for gold coated structure with inner coating diameter of d1/2.5μm @ 1.72μm.

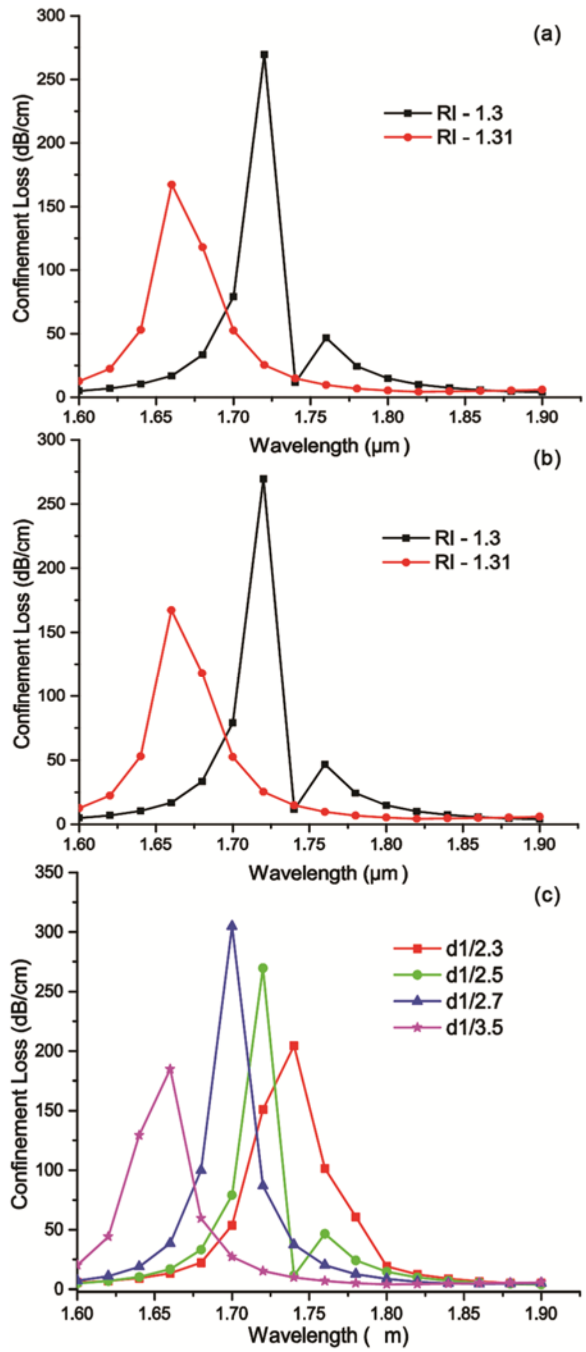

Fig. 7 — (a) Confinement loss spectra of gold coated HCPCF sensor for analyte RI variation from 1.3 to 1.31, (b) comparison of peak losses between gold filled and gold coated structures and (c) variation in confinement loss as the coating thickness increases from d1/2.3 to d1/2.7 (inner air hole diameter) .

4 Conclusions

A gold filled nanowire HCPCF biosensor is designed and simulated and its analysis have been carried out using finite element method to measure the loss spectrum and sensitivity. The proposed sensor has a peak confinement loss of 233.35 dB/cm at 1.64 μm and 210 dB/cm at 1.58 μm for core analyte RI values of 1.3 and 1.31 respectively. The spectral sensitivity is calculated to be 7000 $nmRIU^{-1}$. The effect of increasing the value of Bezier polygon parameter is discussed and is found that it is directly proportional to the loss factor though it induces a blue shift in resonance wavelength. Increasing the polygon parameter from 3.5 to 4, increases the confinement loss from 207.35 dB/cm to 233.35 dB/cm and the peak resonance wavelength shifts from 1.71 μm to 1.64 μm. The modified gold coated HCPCF structure is observed to exhibit greater confinement loss of 269.64 dB/cm at 1.72 μm for analyte with RI of 1.3 and thus exhibiting an increased resonance compared to gold filled structure. The loss factor for gold coated structure with inner air hole diameter $d_1/2.5$ and $d_1/2.7$ are 269.64 dB/cm at 1.72 μm and 304.7 dB/cm at 1.7 μm respectively. The numerical data reveal that a relatively better performance is achieved for increased coating thickness.

References

1 Homola J, *Anal Bioanal Chem,* 377 (2003) 528.
2 Tanya W B, *Meas Sci Technol,* 12 (2001) 854.
3 Otupiri R, Akowuah E, Haxha S, Ademgil H, Abdel Malek F & Aggoun A, *IEEE Photonics J*, 6 (2014) 1.
4 Akowuah E K, Gorman T, Ademgil H, Haxha S, Robinson G K & Oliver, *IEEE J Quantum Electron*, 48 (2012) 1403.
5 Bo Leidberg, Claes Nylander & Ingemar Lunstrom, *Sens Actuators*, 4 (1983) 299.
6 Zhou C, Zhang Y, Xia L & Liu D, *Opt Commun*, 285 (2012) 2466.
7 Shuai B, Xia L, Zhang Y & Liu D, *Opt Express*, 20 (2012) 5974.
8 Ying Lu, Cong-Jing Hao, Bao-Qun Wu, Mayilamu Musideke, Liang-Cheng Duan, Wu-Qi Wen & Jian-Quan Yao, *Sensors*, 13 (2012) 956.
9 X Jiang T, Euser G, Abdolvand A, Babic F, Tani F, Joly N Y, Travers J C & Russell J, *Opt Express*, 19 (2011) 15438.
10 Nannan Luan, Ran Wang, Wenhua LV, Jianquan Yao, *Opt Express*, 23 (2015) 8576.
11 Tushar Biswas, Subir Majumder, Mrinmay Pal & Shyamal K Bhadra, *Springer Proc Phys,* 166 (2015).
12 Li W , Cheng H, Xia M & Yang K, *Sens. Actuators A Phys,* 199 (2013) 260.
13 Sun Dandan, Tuan Guo, Yang Ran, Yunyun Huang & Bai-Ou Guan, *Biosens Bioelectron*, 61 (2014) 541.
14 Soylemez, Saniye, Yasemin A Udum, Melis Kesik, Cevher Gündoğdu Hızlıateş, Yavuz Ergun & Levent Toppare, *Sens Actuators B,* 212 (2015) 425.
15 Luo B, Yan Z, Sun Z, Li J & Zhang L, Opt *Express*, 22 (2014) 30571.
16 Rifat A A, Amouzad Mahdiraji G, Shee Y G, Jubayer Shawon & Mahamd Adikan F R, *Procedia Eng,* 140 (2016) 1.
17 Ahmed E Khalil, Ahmed H El-Saeed, Mohamed A Ibrahim, Mohamed E Hashish, Mohammed R Abdelmonem, Mohamed Farhat O Hameed, Mohammad Y Azab & S S A Obayya, *Opt Quantum Electron*, 50 (2018) 158.
18 Yong Zhao, Rui-jie Tong, Feng Xia & Yun Peng, *Biosens Bioelectron,* 142 (2019) 111505.
19 Ayyanar N, Thavasi Raja G, Sharma M & Sriram Kumar D, *IEEE Sens J,* 18 (2018) 7093.
20 Joannopoulos J D, Johnson S G, Winn J N & Meade R D, Photonic crystals molding the flow of light (Princeton University Press.: Princeton and oxford) 2nd Edn, ISBN:978-0-691-12456-8, 2007, p.165.
21 Kang Xie, Wei Zhang, Allan D Boardman, Haiming Jiang, Zhijia Hu, Yong Liu, Ming Xie, Qiuping Mao, Lei Hu, Qian Li, Tianyu Yang, Fei Wen & Erlei Wang, *Light Sci Appl*, 4 (2015) sp - e304.
22 Guangyao Wang, Shuguang Li, Gowen An, Xinyu Wang, Yunyan Zhao, Wan Zhang & Hailiang Chen, *Opt Quantum Electron,* 48 (2015).
23 Yogalakshmi S, Selvendran S & Sivanantha Raja A, *Laser Phys,* 26 (2016) 056201.
24 Jianchen Zi, Shuguang Li, Hailiang Chen, Jianshe Li & Hui Li Zi, *Plasmonics*, 11 (2016) 65.